COSMOCHEMISTRY

The Moon-forming impactor Theia originated from the inner Solar System

Timo Hopp[1,2]*, Nicolas Dauphas[1,3], Maud Boyet[4], Seth A. Jacobson[5], Thorsten Kleine[2]

The Moon formed from a giant impact of a planetary body, called Theia, with proto-Earth. It is unknown whether Theia formed in the inner or outer Solar System. We measured iron isotopes in lunar samples, terrestrial rocks, and meteorites representing the isotopic reservoirs from which Theia and proto-Earth might have formed. Earth and the Moon have indistinguishable mass-independent iron isotopic compositions; both define one end of the range measured in meteorites. Combining our results with those for other elements, we performed mass balance calculations for Theia and proto-Earth. We found that all of Theia and most of Earth's other constituent materials originated from the inner Solar System. Our calculations suggest that Theia might have formed closer to the Sun than Earth did.

The Moon is thought to have formed following a giant impact between a Mars-sized body, called Theia, and proto-Earth (*1*, *2*). Most models of this process predict that the Moon is predominantly composed of material derived from Theia. If Theia was isotopically distinct from proto-Earth, then this would produce an isotopic difference between the Moon and Earth's mantle. Such isotopic differences between planetary objects can arise through radioactive decay, isotopic fractionation processes, and the uneven distribution of presolar materials in the Solar System's protoplanetary disk. The latter can indicate a planet's provenance by comparison with noncarbonaceous (NC) and carbonaceous chondrite (CC) meteorites, which are thought to represent the inner and outer Solar System, respectively (*3*–*6*). Determining the nucleosynthetic isotopic composition of Theia could therefore indicate whether it formed in the inner (*7*–*9*) or outer Solar System (*10*–*12*).

Measurements of lunar samples have shown that Earth and the Moon have similar mass-independent isotopic compositions for all measured elements, including oxygen (O), calcium (Ca), titanium (Ti), chromium (Cr), zirconium (Zr), and tungsten (W) (*8*, *13*–*19*). Several explanations have been proposed for this isotopic similarity: (i) Theia and proto-Earth might have formed in the same region of the protoplanetary disk (*20*); (ii) the Moon could be derived predominantly from the mantle of proto-Earth (*13*, *21*); (iii) the Moon and Earth's mantle incorporated equal proportions of material from Theia and proto-Earth (*22*); or (iv) the Moon and Earth's mantle compositions were homogenized owing to extensive mixing and isotopic exchange following the giant impact (*23*, *24*). The lack of measurable isotopic differences and uncertainty over which process caused this have prevented a determination of Theia's formation region.

[1]Department of the Geophysical Sciences, The University of Chicago, Chicago, IL, USA. [2]Max-Planck-Institut für Sonnensystemforschung, Göttingen, Germany. [3]Department of Earth and Planetary Sciences, The University of Hong Kong, Hong Kong, China. [4]Laboratoire Magmas et Volcans, Université Clermont Auvergne, Centre National de la Recherche Scientifique, Institut de Recherche pour le Développement, Observatoire de Physique du Globe de Clermont-Ferrand, Clermont-Ferrand, France. [5]Department of Earth and Environmental Sciences, Michigan State University, East Lansing, MI, USA. ***Corresponding author. Email: hopp@mps.mpg.de**

Iron isotopic measurements

We measured the iron (Fe) isotopic compositions of 15 terrestrial rocks, 6 lunar samples retrieved by the Apollo missions, and 20 undifferentiated NC meteorites [enstatite chondrites (ECs), ordinary chondrites (OCs), and Rumuruti-type chondrites]. After purification of Fe by ion exchange chromatography, the isotopic measurements were conducted using multicollector inductively coupled plasma mass spectrometry (*25*). The data are reported as μ^{54}Fe and μ^{58}Fe values (table S1), which express the ^{54}Fe/^{56}Fe and ^{58}Fe/^{56}Fe ratios in the sample, normalized to a fixed ^{57}Fe/^{56}Fe, as deviations in parts per million relative to a synthetic standard solution: $\mu^{i}\mathrm{Fe} = [(^{i}\mathrm{Fe}/^{56}\mathrm{Fe})_{\mathrm{sample}}/(^{i}\mathrm{Fe}/^{56}\mathrm{Fe})_{\mathrm{standard}} - 1] \times 10^{6}$, where i represents the atomic mass of each measured isotope.

The Fe isotopic compositions of all the terrestrial samples are indistinguishable (Fig. 1A), with average values of $\mu^{54}\mathrm{Fe} = 0 \pm 1$ and $\mu^{58}\mathrm{Fe} = +1 \pm 3$; all uncertainties are 95% confidence intervals. We take this composition to be representative of Earth's mantle, referred to as the bulk silicate Earth (BSE). The Fe isotopic compositions of 14 ECs are indistinguishable from each other (Fig. 1B), with average $\mu^{54}\mathrm{Fe} = +6 \pm 1$ and $\mu^{58}\mathrm{Fe} = 0 \pm 2$. This μ^{54}Fe difference between ECs and the BSE indicates that ECs cannot be the sole isotopic reservoir from which Earth is derived.

For the six lunar samples, we found that μ^{54}Fe and μ^{58}Fe are anticorrelated (Fig. 1C). This is consistent with exposure of some of the samples to galactic cosmic rays (GCRs), which causes secondary neutron capture that is predicted to produce a negative correlation (*25*–*27*). Previous measurements of meteorites with low GCR exposure displayed no variations in μ^{58}Fe values (*6*, *27*, *28*). We therefore expect the μ^{58}Fe value of the Moon's mantle [the bulk silicate Moon (BSM)], prior to GCR exposure, to be zero and attribute all the μ^{58}Fe variations among the lunar samples to GCR effects. Three samples have similar μ^{54}Fe and near-zero μ^{58}Fe values, indicating that these are unaffected by GCR; their weighted average is $\mu^{54}\mathrm{Fe} = +2 \pm 3$ (*25*). Thus, the μ^{54}Fe values of the BSM ($+2 \pm 3$) and BSE (0 ± 1) are indistinguishable.

Unsampled constituents of Earth and the Moon

The NC meteorites exhibit correlations between the isotopic anomalies of multiple elements with different geochemical behavior. For Fe and Zr, the BSE lies beyond the range of measured compositions of meteorites but on the same correlation line (Fig. 2) (*29*–*31*); therefore, the BSE cannot be explained by mixtures of NC and CC meteorites. There are several potential explanations for the composition of BSE lying at one end of the range observed in meteorites, including that (i) proto-Earth and Theia had the same isotopic composition and both incorporated material that is not recorded in meteorites; (ii) proto-Earth's mantle (PEM) had a composition not recorded in meteorites, whereas Theia's isotopic composition was within the range of meteorites; or (iii) Theia had an isotopic composition not recorded in meteorites and the PEM's isotopic composition was within the meteoritic range.

The isotopic composition of BSE for elements with different geochemical behavior reflects the materials that accreted during different stages of Earth's growth (*32*). For lithophile (rock-loving, predominantly in the mantle and crust) elements, such as Zr, the isotopic composition of BSE is determined by Earth's full accretion history (fig. S1). For moderately siderophile (metal-loving, predominantly in the core) elements, such as Fe and molybdenum (Mo), the isotopic composition of BSE reflects the final ~40 and ~10%, respectively, of material accreted by Earth, because any of those elements that were contained in material that was accreted earlier will have partitioned into the core (figs. S1 and S2) (*32*). For highly siderophile elements, such as ruthenium (Ru), their abundances in the BSE were predominantly set after core formation ceased, during the final ~0.5% of Earth's accretion (known as late accretion or the late veneer) (*33*, *34*). Lithophile and

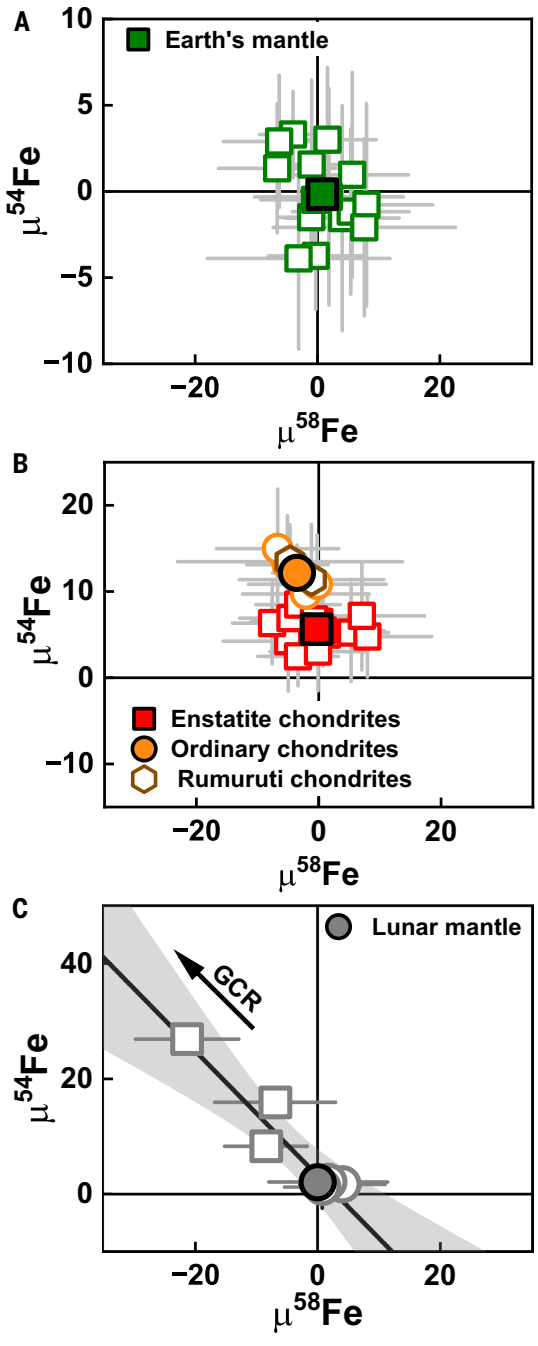

Fig. 1. Fe isotopic compositions of terrestrial rocks, lunar rocks, and meteorites. $\mu^{54}Fe$ and $\mu^{58}Fe$ data are from our laboratory measurements (table S1). Error bars indicate 95% confidence intervals. Horizontal and vertical black lines represent the composition of the reference standard solution (zero by definition). Open symbols represent individual samples and solid symbols the calculated average compositions. (**A**) Samples of terrestrial rocks have indistinguishable Fe isotopic compositions, with average $\mu^{54}Fe = 0 \pm 1$ and $\mu^{58}Fe = +1 \pm 3$. (**B**) Samples of undifferentiated NC meteorites (ECs, OCs, and Rumuruti-type chondrites) have nonzero isotopic anomalies in $\mu^{54}Fe$. (**C**) Lunar samples have anticorrelated values of $\mu^{54}Fe$ and $\mu^{58}Fe$. The black regression line (shaded region represents the 95% confidence intervals) is consistent with exposure of the samples to GCRs, which is expected to move the isotopic composition in the direction indicated by the black arrow. Open squares represent samples that were affected by GCRs and so were discarded from our analysis. Three lunar samples (open circles) have $\mu^{58}Fe$ consistent with zero and similar $\mu^{54}Fe$ values; their weighted average, $\mu^{54}Fe = +2 \pm 3$ (solid circle), was taken to reflect the BSM.

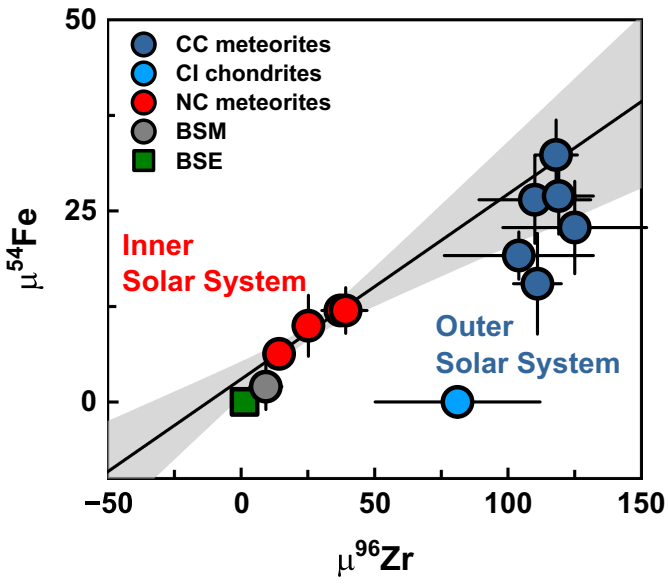

Fig. 2. Fe and Zr isotopic compositions of Earth's mantle, the Moon, and meteorites. $\mu^{54}Fe$ and $\mu^{96}Zr$ are shown for different sample types (see legend); data are from this study and previous work (table S2) (*29*, *30*, *49*). Error bars represent 95% confidence intervals. The black line shows a linear regression fitted to the NC data (red circles), with the gray shaded region indicating the 95% confidence intervals. Earth's mantle (BSE, green square) and the Moon's mantle (BSM, gray circle) are outside the range of NC meteorites and furthest away from CC meteorites.

highly siderophile elements predominantly record earlier and later stages of Earth's accretion, respectively. Because the formation of the Moon occurred near the end of Earth's accretion process (*1*, *2*), Theia likely supplied a considerable amount of siderophile elements to the BSE. If proto-Earth and Theia were isotopically distinct, then we would expect the isotopic composition of a siderophile element in BSE to be closer to that of Theia than for a lithophile element. Comparing the isotopic anomalies of siderophile and lithophile elements in the BSE and BSM can therefore constrain the isotopic composition of Theia.

Mass-balance calculations

Most giant impact models predict that there is no isotopic homogenization and that the Moon predominantly consists of material from Theia (*1*, *2*). In this case, which we refer to as the canonical model, the isotopic similarity between the BSE and BSM requires that Theia and proto-Earth had similar isotopic compositions, implying that both formed in the same region of the protoplanetary disk (*8*, *16*, *20*) (figs. S3 and S4). However, dynamical models of planet formation predict that Earth accreted material that originated from multiple regions of the disk (*35*). Given the measured isotopic variations among meteorites and planets, this makes it unlikely that Theia and proto-Earth had identical compositions (*3*, *15*, *23*).

In the canonical model, the BSE and the BSM are also expected to have different ^{182}W signatures, caused by radioactive decay of hafnium-182 (^{182}Hf). Variations in ^{182}W reflect the timescales and conditions of core formation, which were likely different for Theia and proto-Earth because of their different accretion history (*36*). However, only a small difference in ^{182}W between Earth and Moon rocks has been measured, which can be explained by either radioactive decay in the Moon (*37*) or disproportional late accretion to Earth and the Moon (*18*, *19*). It has therefore been argued that the BSE and BSM had indistinguishable ^{182}W signatures immediately after the giant impact. This is a possible

but unlikely outcome of canonical giant impact models (*38*, *39*). Because ^{182}W variations are produced by radioactive decay, this argument holds regardless of whether proto-Earth and Theia originated in the same region of the disk.

Alternative (noncanonical) giant impact scenarios have been proposed to account for the isotopic similarity between Earth and the Moon. These models either produce the Moon predominantly from PEM material (*13*, *21*) or enable isotopic homogenization of the BSE and BSM (*23*, *24*). These scenarios do not require PEM and Theia to have had similar isotopic compositions but do imply that measurements of lunar samples provide no direct information on Theia's original isotopic composition.

For different assumed isotopic compositions ${}^{i}E$ (where E represents an arbitrary element) of the PEM, we determined possible isotopic compositions of Theia through mass-balance calculations. We used the measured composition of Earth's mantle, $\mu^{i}E_{BSE}$, as a proxy for both the present-day BSE and the Moon (*25*). Then mass balance requires

$$\mu^{i}E_{Theia} = \frac{\mu^{i}E_{BSE} - \mu^{i}E_{PEM}(1-x_E)}{x_E} \quad \text{(Eq. 1)}$$

where $\mu^{i}E_{Theia}$ and $\mu^{i}E_{PEM}$ are the model isotopic compositions of Theia and PEM, and x_E is the mass fraction of element E in the BSE that was delivered by Theia. We rearranged Eq. 1 to calculate $\mu^{i}E_{PEM}$ for different assumed values of $\mu^{i}E_{Theia}$:

$$\mu^{i}E_{PEM} = \frac{\mu^{i}E_{BSE} - \mu^{i}E_{Theia}x_E}{1-x_E}. \quad \text{(Eq. 2)}$$

The value of x_E depends on the mass of the impactor. For siderophile elements, x_E also depends on the assumed redox states of proto-Earth and Theia, which affects the partitioning of siderophile elements between the silicate mantle and metallic core, and the degree to which Theia's core equilibrated with PEM (figs. S1 and S2) (*25*, *32*). To cover the range of potential x_E values, we calculated $\mu^{i}E_{Theia}$ and $\mu^{i}E_{PEM}$ separately for several impactor masses: a small Theia, 5% of Earth's mass (*21*); a canonical model, with Theia having 10% of Earth's mass (*1*, *2*); and a large Theia, 50% of Earth's mass (*22*) (table S3). For the small and canonical impactors, x_E was estimated from a previous model (*32*), assuming that Theia was the last giant impact on Earth (figs. S1 and S2). For the large (half-Earth) impactor (fig. S5), we assumed that 50% of all elements in BSE came from Theia (*22*).

Our mass balance calculations only require measurements of the BSE composition (Eqs. 1 and 2). We therefore included Mo in our model, even though its isotopic signature has not been measured in lunar samples. Because Mo is more siderophile than Fe, it records the final ~10% of Earth's accretion, so a substantial fraction of Mo in the BSE could come from Theia (*12*). Some of the Mo in BSE was delivered by late accretion after the giant impact, likely by NC material (*34*, *40*, *41*). To account for this, we corrected the BSE Mo isotopic composition using the fraction of Mo delivered by late accretion, which we calculated to be $x_{Mo\text{-}LV} = 0.16$ (*25*), and assuming an enstatite chondrite-like isotopic composition for the late veneer (*25*). This correction is small, shifting $\mu^{94}Mo$ of the BSE from $+4 \pm 6$ to -2 ± 7; we adopted the corrected value in the mass balance calculations. If we instead assume an Ivuna-type carbonaceous chondrite (CI) isotopic composition of the late accreted material, the results change only slightly (table S4).

Determining Theia's isotopic origin

Our mass balance calculations provide the composition of PEM for different assumed compositions and masses of Theia. In most cases, we found that PEM is required to have had negative anomalies for Fe, Zr, and Mo (Fig. 3 and fig. S5). Such negative anomalies have not been measured in meteorites. The calculated PEM composition is closer to meteoritic compositions when the impactor is small and has CI- or EC-like compositions. For a small Theia with CI-like composition, we calculated that PEM had $\mu^{54}Fe = 0 \pm 1$ and $\mu^{96}Zr = -3 \pm 3$, whereas for a small EC-like Theia, we obtained $\mu^{54}Fe = -1 \pm 1$ and $\mu^{96}Zr = 0 \pm 2$. These values are indistinguishable from the current BSE composition. For Mo, we calculated that PEM had $\mu^{94}Mo = -98 \pm 49$ and -50 ± 18 for a small CI-like and EC-like Theia, which are both distinct from BSE (Fig. 3E).

We also calculated the composition of Theia for different assumed PEM compositions (Fig. 4 and fig. S5). If proto-Earth's composition was within the meteoritic range, then Theia must have had a composition outside the meteoritic range, with negative $\mu^{54}Fe$, $\mu^{96}Zr$, and $\mu^{94}Mo$ values. For CI- or CC-like isotopic compositions of PEM, the calculated Fe and Zr isotopic compositions of Theia would be highly anomalous, far outside the range measured for meteorites. For example, CI chondrites have a similar Fe isotopic composition to Earth's mantle (*42*) but large positive $\mu^{96}Zr$ anomalies (*43*, *44*). Therefore, if

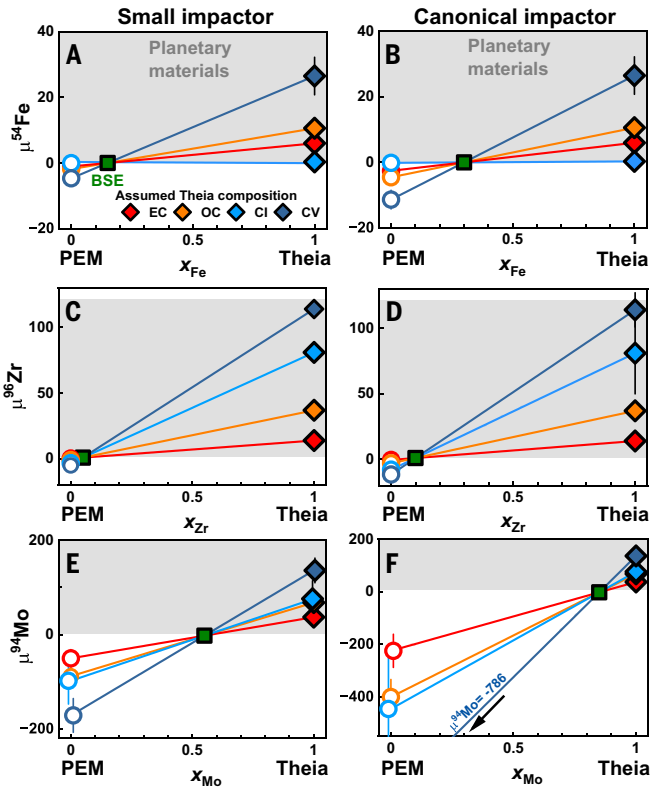

Fig. 3. Mass-balance calculations for different compositions of Theia. Results are shown for (**A** and **B**) Fe, (**C** and **D**) Zr, and (**E** and **F**) Mo. Each panel shows the isotopic composition $\mu^{i}E$ as a function of the mass fraction of element E in the BSE that was delivered by Theia (x_E) under two scenarios: [(A), (C), and (E)] a small 0.05–Earth masses impactor and [(B), (D), and (F)] a canonical 0.1–Earth masses impactor. Error bars indicate 95% confidence intervals. The colored lines follow the mass balance between the assumed isotopic composition of Theia (filled diamonds), the measured isotopic composition of Earth's mantle (BSE, filled green squares), and the calculated isotopic composition of PEM (open circles). The shaded areas indicate the range of isotopic compositions measured in planetary materials (table S2). For Theia, isotopic compositions similar to NC meteorite groups (EC and OC) and CC meteorite groups [CI and Vigarano-type carbonaceous chondrites (CV)] are assumed (see legend). Results for a 0.5–Earth mass impactor are shown in fig. S5. The calculated compositions for each scenario are summarized in table S3.

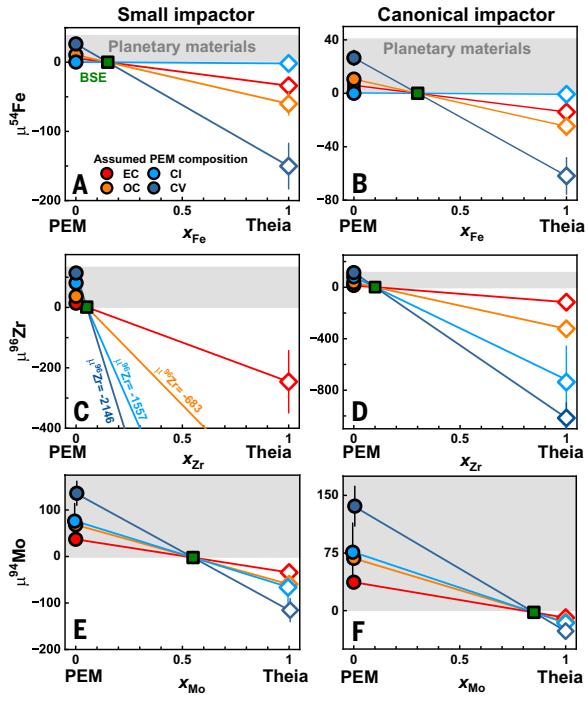

Fig. 4. Mass-balance calculations for different PEM compositions. (**A** to **F**) Same as Fig. 3, except the isotopic composition of Theia was calculated by using the measured isotopic composition of BSE (solid green square) and assuming that PEM (filled circles) had similar isotopic composition to that of different meteorite groups (see legend). The calculated compositions of the different scenarios are summarized in table S3.

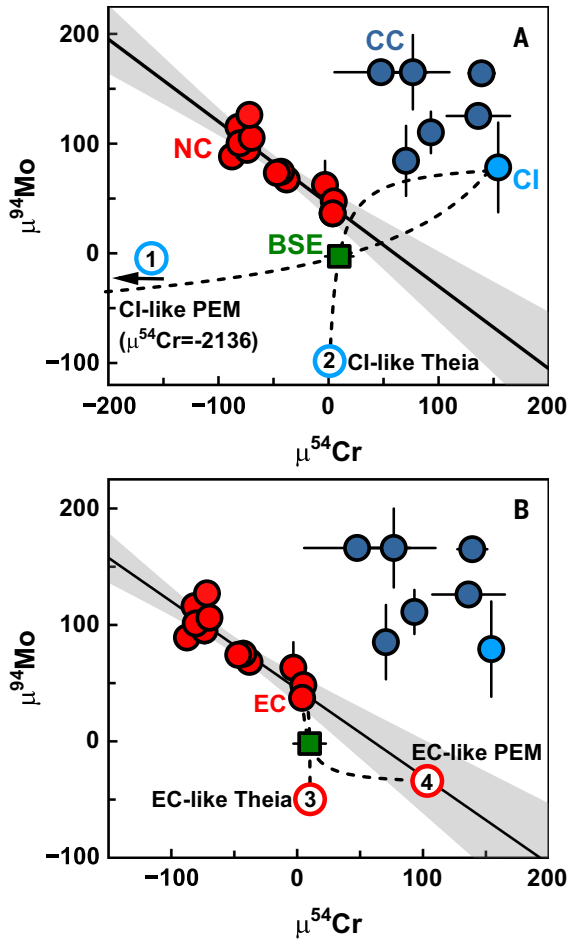

Fig. 5. Mo and Cr isotopic compositions of Earth's mantle and meteorites. Data points in both panels show previous measurements of μ^{94}Mo and μ^{54}Cr for different sample types (table S2) (*29*, *30*, *49*). Nonmagmatic Fe meteorites have been excluded, because Mo and Cr might have different origins in those meteorites (see supplementary text). The black line shows a linear regression fitted to the NC data (red circles). Error bars and the gray shaded region represent 95% confidence intervals. The BSE (green square) is below the correlation defined by NC meteorites. (**A**) Results of the mass-balance calculations for a small impactor scenario, which used the measured composition of the BSE and assumed either a CI-like PEM or Theia (open blue circles labeled 1 and 2). The black arrow indicates that scenario 1 is located beyond the plotted region, at μ^{54}Cr = −2136. The dashed lines represent mixing curves between CI composition (light blue solid circle) and the calculated compositions of Theia and PEM in each scenario. (**B**) Results of the mass-balance calculations for a small impactor scenario assuming an EC-like composition of Theia or PEM (red circles labeled 3 and 4). The calculated compositions for each of the scenarios are summarized in table S3.

PEM had a CI-like isotopic composition, then it would require Theia to be extremely anomalous, with μ^{96}Zr between −81 (for a half-Earth impactor) and −1557 (for a small impactor). By contrast, an NC-like PEM generally implies much less anomalous Theia compositions for Fe, Zr, and Mo (Fig. 4 and table S3). In all our calculations, some exotic material (material with an isotopic composition outside the range measured in meteorites) is always required, but it is less exotic if proto-Earth was similar to NC meteorites and close in composition to the BSE.

We obtained more stringent constraints by examining multiple elements simultaneously. Isotopic anomalies are correlated among NC materials, indicating that they arose through two-component mixing (*30*, *45*). One of these components is not present in measured meteorites, but must form an endmember of the NC correlation, characterized by negative μ^{54}Fe, μ^{96}Zr, and μ^{94}Mo but positive μ^{54}Cr values (*29*, *30*). In plots of μ^{94}Mo versus μ^{54}Cr (Fig. 5) and μ^{54}Fe versus μ^{54}Cr (fig. S6), the BSE is located below the NC correlation and away from CC and CI meteorites (*29*). We interpreted these offsets as due to the different siderophile behaviors of Cr, Fe, and Mo, leading to different fractional contributions from Theia (x_E values).

Figure 5 shows the compositions of different hypothetical components that would be required to explain the BSE composition in the small impactor scenario, which provides the fewest constraints on Theia when examining individual elements separately (Figs. 3 and 4). If either Theia or the PEM had CC- or CI-like compositions, then the hypothetical component would need to be far on the other side of the NC correlation, in a region that has not been measured in meteorites (Fig. 5A). If PEM had an EC-like composition, then the calculated Theia composition falls on an extrapolation of the NC correlation. The μ^{94}Mo versus μ^{54}Cr mixing curve for an EC-like PEM with this hypothetical Theia passes through the composition of BSE (Fig. 5B). In this case, the offset of the BSE away from the NC correlation is due to Theia's differing contributions to the BSE's Cr and Mo inventories (*29*).

Mo isotopic variations among meteorites primarily arise from varying amounts of material produced by the slow neutron capture process (*s*-process) (*46*, *47*), with additional variations from the rapid neutron capture process (*r*-process), which contributed more to the CC reservoir than to the NC reservoir (*5*). Mo in the BSE also has a small *r*-process enrichment compared to NC meteorites, indicating a small contribution from CC material (*11*, *12*). This CC contribution can be reconciled with an NC origin of Theia if the impactor was small or if there was little mixing between Theia's core and PEM; in this case,

the CC material would have been delivered shortly before the Moon-forming impact (*11*, *25*).

The most plausible scenario is that both proto-Earth and Theia were predominantly formed from NC material and that Theia was likely more enriched in *s*-process material than were NC meteorites and the BSE. It has been proposed that the measured *s*-process variation among NC bodies reflects a heliocentric gradient in the inner Solar System (*29*, *30*). If that is correct, then our preferred scenario implies that Theia formed closer to the Sun than did most of the material that accreted to form Earth. Ru isotopic compositions of some ancient Earth rocks display an enrichment in *s*-process nuclides, which has been interpreted as reflecting the Ru isotopic composition of Earth's mantle prior to late accretion (*48*). Some of this Ru could derive from the Moon-forming impactor, consistent with our finding of an *s*-process–enriched composition of Theia.

REFERENCES AND NOTES

1. R. M. Canup, E. Asphaug, *Nature* **412**, 708–712 (2001).
2. R. M. Canup, *Icarus* **168**, 433–456 (2004).
3. P. H. Warren, *Earth Planet. Sci. Lett.* **311**, 93–100 (2011).
4. T. S. Kruijer, C. Burkhardt, G. Budde, T. Kleine, *Proc. Natl. Acad. Sci. U.S.A.* **114**, 6712–6716 (2017).
5. G. Budde *et al.*, *Earth Planet. Sci. Lett.* **454**, 293–303 (2016).
6. T. Hopp *et al.*, *Sci. Adv.* **8**, eadd8141 (2022).
7. S. J. Desch, K. L. Robinson, *Chem. Erde* **79**, 125546 (2019).
8. W. Akram, M. Schönbächler, *Earth Planet. Sci. Lett.* **449**, 302–310 (2016).
9. M. M. M. Meier, A. Reufer, R. Wieler, *Icarus* **242**, 316–328 (2014).
10. M. Schönbächler, R. W. Carlson, M. F. Horan, T. D. Mock, E. H. Hauri, *Science* **328**, 884–887 (2010).
11. G. Budde, C. Burkhardt, T. Kleine, *Nat. Astron.* **3**, 736–741 (2019).
12. T. Hopp, G. Budde, T. Kleine, *Earth Planet. Sci. Lett.* **534**, 116065 (2020).
13. J. Zhang, N. Dauphas, A. M. Davis, I. Leya, A. Fedkin, *Nat. Geosci.* **5**, 251–255 (2012).
14. U. Wiechert *et al.*, *Science* **294**, 345–348 (2001).
15. E. D. Young *et al.*, *Science* **351**, 493–496 (2016).
16. B. Mougel, F. Moynier, C. Göpel, *Earth Planet. Sci. Lett.* **481**, 1–8 (2018).
17. M. Schiller, M. Bizzarro, V. A. Fernandes, *Nature* **555**, 507–510 (2018).
18. T. S. Kruijer, T. Kleine, M. Fischer-Gödde, P. Sprung, *Nature* **520**, 534–537 (2015).
19. M. Touboul, I. S. Puchtel, R. J. Walker, *Nature* **520**, 530–533 (2015).
20. N. Dauphas, C. Burkhardt, P. H. Warren, T. Fang-Zhen, *Philos. Trans. A Math. Phys. Eng. Sci.* **372**, 20130244 (2014).
21. M. Ćuk, S. T. Stewart, *Science* **338**, 1047–1052 (2012).
22. R. M. Canup, *Science* **338**, 1052–1055 (2012).
23. K. Pahlevan, D. J. Stevenson, *Earth Planet. Sci. Lett.* **262**, 438–449 (2007).
24. S. J. Lock *et al.*, *J. Geophys. Res. Planets* **123**, 910–951 (2018).
25. Materials and methods are available as supplementary materials.
26. D. L. Cook, I. Leya, M. Schönbächler, *Meteorit. Planet. Sci.* **55**, 2758–2771 (2020).
27. N. Hopp, N. Dauphas, F. Spitzer, C. Burkhardt, T. Kleine, *Earth Planet. Sci. Lett.* **577**, 117245 (2022).
28. D. L. Cook, B. S. Meyer, M. Schönbächler, *Astrophys. J.* **917**, 59 (2021).
29. C. Burkhardt *et al.*, *Sci. Adv.* **7**, eabj7601 (2021).
30. F. Spitzer *et al.*, *Astrophys. J. Lett.* **898**, L2 (2020).
31. N. Dauphas, A. M. Davis, B. Marty, L. Reisberg, *Earth Planet. Sci. Lett.* **226**, 465–475 (2004).
32. N. Dauphas, *Nature* **541**, 521–524 (2017).
33. D. C. Rubie *et al.*, *Science* **353**, 1141–1144 (2016).
34. M. Fischer-Gödde, T. Kleine, *Nature* **541**, 525–527 (2017).
35. J. E. Chambers, *Icarus* **152**, 205–224 (2001).
36. R. A. Fischer, F. Nimmo, *Earth Planet. Sci. Lett.* **499**, 257–265 (2018).
37. M. M. Thiemens, P. Sprung, R. O. C. Fonseca, F. P. Leitzke, C. Münker, *Nat. Geosci.* **12**, 696–700 (2019).
38. R. A. Fischer, N. G. Zube, F. Nimmo, *Nat. Commun.* **12**, 35 (2021).
39. T. S. Kruijer, T. Kleine, *Earth Planet. Sci. Lett.* **475**, 15–24 (2017).
40. E. A. Worsham, T. Kleine, *Sci. Adv.* **7**, eabh2837 (2021).
41. K. R. Bermingham, R. J. Walker, *Earth Planet. Sci. Lett.* **474**, 466–473 (2017).
42. M. Schiller, M. Bizzarro, J. Siebert, *Sci. Adv.* **6**, eaay7604 (2020).
43. J. Render, G. A. Brennecka, C. Burkhardt, T. Kleine, *Earth Planet. Sci. Lett.* **595**, 117748 (2022).
44. W. Akram, M. Schönbächler, S. Bisterzo, R. Gallino, *Geochim. Cosmochim. Acta* **165**, 484–500 (2015).
45. C. Burkhardt, N. Dauphas, U. Hans, B. Bourdon, T. Kleine, *Geochim. Cosmochim. Acta* **261**, 145–170 (2019).
46. N. Dauphas, B. Marty, A. L. Reisberg, *Astrophys. J.* **565**, 640–644 (2002).
47. C. Burkhardt *et al.*, *Earth Planet. Sci. Lett.* **312**, 390–400 (2011).
48. M. Fischer-Gödde *et al.*, *Nature* **579**, 240–244 (2020).
49. N. Dauphas, T. Hopp, D. Nesvorný, *Icarus* **408**, 115805 (2024).

ACKNOWLEDGMENTS

We thank CAPTEM and R. A. Ziegler for providing the Apollo lunar samples; H. Becker (FU Berlin), N. T. Arndt (CNRS, Grenoble), and B. Marty (CNRS, Nancy) for providing the terrestrial samples; and the Robert A. Pritzker Center for Meteoritics at the Field Museum of Natural History (Chicago), the Smithsonian National Museum for Natural History (Washington, DC), the Institut für Planetologie Münster, and the National Aeronautics and Space Administration (NASA) for providing the meteorite samples. US Antarctic meteorite samples were recovered by the Antarctic Search for Meteorites (ANSMET) program, which has been funded by the National Science Foundation (NSF) and NASA, and characterized and curated by the Department of Mineral Sciences of the Smithsonian Institution and the Astromaterials Curation Office at the NASA Johnson Space Center. **Funding:** N.D. was supported by NASA grants 80NSSC20K1409, 80NSSC23K1022, 80NSSC21K0380, 80NSSC20K0821, and 80NSSC23K1163; NSF grant EAR-2001098; and Department of Energy grant DE-SC0022451. T.K. was supported by the Deutsche Forschungsgemeinschaft (DFG) project ID 263649064 and the European Research Council advanced grant no. 101019380. **Author contributions:** T.H. and N.D. conceived the study. T.H., N.D., and T.K. interpreted the data. T.H. measured the Fe isotopic compositions of the samples. T.K. and M.B. provided samples and discussed the interpretation. T.H. and N.D. wrote the manuscript, with feedback from T.K., M.B., and S.A.J. **Competing interests:** The authors declare that they have no competing interests. **Data and materials availability:** The Fe isotopic data are provided in table S1 and data S1. The isotopic data compiled from the literature are listed (with references) in table S2 and data S2. The results of our mass balance calculations are listed in tables S3 and S4. All lunar, meteorite, terrestrial, and standard samples are archived and available for further study; full details of the sample origins and how readers may request access to them are provided in the supplementary materials.

SUPPLEMENTARY MATERIALS

science.org/doi/10.1126/science.ado0623
Materials and Methods; Supplementary Text; Figs. S1 to S8; Tables S1 to S6; References (*50*–*111*); Data S1 and S2

Submitted 15 January 2024; accepted 19 September 2025

10.1126/science.ado0623